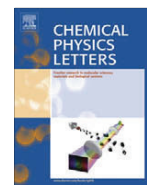




Contents lists available at ScienceDirect

Chemical Physics Letters

journal homepage: [www.elsevier.com/locate/cplett](http://www.elsevier.com/locate/cplett)

## Reaction dynamics of the phenyl radical with 1,2-butadiene

Xibin Gu<sup>a</sup>, Fangtong Zhang<sup>a</sup>, Ralf I. Kaiser<sup>b,\*</sup>, Vadim V. Kislov<sup>b</sup>, Alexander M. Mebel<sup>b</sup><sup>a</sup> Department of Chemistry, University of Hawai'i at Mānoa, Honolulu, HI 96822, United States<sup>b</sup> Department of Chemistry and Biochemistry, Florida International University, Miami FL 33199, United States

### ARTICLE INFO

#### Article history:

Received 19 March 2009

In final form 15 April 2009

Available online 18 April 2009

### ABSTRACT

The crossed beams reaction of the phenyl radical ( $C_6H_5$ ) with 1,2-butadiene ( $CH_3HCCCH_2$ ) was studied under single collision at two collision energies. The crossed beams data were combined with electronic structure calculations on the  $C_{10}H_{11}$  potential energy surface. The reaction was found to follow indirect scattering dynamics via an addition of the phenyl radical with its radical center to the sterically favorable C1 atom of the 1,2-butadiene reactant. The initial reaction intermediate decomposed via atomic hydrogen loss to form two  $C_{10}H_{10}$  isomers, 1-phenyl-3-methylallene (**p1**) and 1-phenyl-butyne-2 (**p2**), via tight exit transition states. The results are compared with the crossed beams study of phenyl radicals with a second  $C_4H_6$  isomer, 1,3-butadiene.

Published by Elsevier B.V.

### 1. Introduction

Polycyclic aromatic hydrocarbons (PAHs) [1] and related molecules such as partially (de)hydrogenated [2–4] and ionized PAHs [5,6] are ubiquitous in terrestrial and celestial environments. On Earth, they are generated in combustion processes of fossil fuel as toxic byproducts. Considering the emission rate of 1.6 million tons per year, PAHs and soot are severe air and marine pollutants [7–9], contribute to the global warming, and are considered as air-born toxic chemicals due to their mutagenic [10] and carcinogenic [11–13] character. On the other hand, in the interstellar medium, it is estimated that PAH-like species account for up to 20% of the total cosmic carbon budget [14,15]. They are linked to the unidentified infrared emission bands (UIBs) [16,17] and to the diffuse interstellar bands (DIBs) [18]. Therefore, in interstellar space, PAH-like species are of crucial importance to understand the evolution of carbon-rich environments such as circumstellar envelopes of carbon stars like IRC + 10 216 and planetary nebulae.

Unfortunately, despite the importance of PAHs in combustion processes and in interstellar space, the underlying formation routes are still a subject of an ongoing discussion. In high temperature environments, the phenyl radical ( $C_6H_5$ ) in its  $^2A_1$  electronic ground state is believed to present one of the most critical transient species to trigger PAH formation [19,20] via reaction with unsaturated hydrocarbons through an addition of the radical center of the phenyl radical to the  $\pi$  electronic system of the unsaturated co-reactants [21]. The intermediates either decompose back to the reactants, fragment to the products, isomerize prior to their decomposition, and/or are stabilized at higher pressures via a third-body collision. Recently, we have conducted a systematic

study of the reactions of phenyl radicals with unsaturated hydrocarbons classified as olefines (ethylene [22], propylene [23], 1,3-butadiene [24]), cumulenes (allene [25]), alkynes (acetylene [26], methylacetylene [25]), and aromatic (benzene [27]) utilizing the crossed molecular beams approach. Here we will introduce the reaction of phenyl radicals with a substituted cumulene (1,2-butadiene) to access the important  $C_{10}H_{10}$  potential energy surface (PES) – among them dihydronaphthalene. As an isomer of 1,3-butadiene, extensive theoretical and experimental investigations on the thermal isomerization and (unimolecular) dissociation of 1,2-butadiene have been reported. These involved photolysis [28–30] and pyrolysis experiments [31,32]. But unlike 1,3-butadiene, only a few reactions of 1,2-butadiene have been reported. These are reactions with atoms of hydrogen, carbon, oxygen, and sulfur and with hydroxyl (OH) and methyl ( $CH_3$ ) radicals. The only system studied under single collision conditions is the reaction of atomic carbon with 1,2-butadiene [33]. Most papers suggest that 1,2-butadiene acts as a precursor of small hydrocarbon radicals in pyrolysis processes like propargyl and methyl [32,34–36], which initiate subsequent radical chain reactions to form single or multiple aromatic ring structures. In addition, the mutual isomerization of 1,2-butadiene, 1,3-butadiene, and 2-butyne was shown to be much faster than its decomposition at high temperature [35,36]. Therefore, it is justified to study not only the unimolecular decomposition of these isomers, but also the underlying reaction dynamics as presented here.

### 2. Experimental

A detailed description of the crossed molecular beams machine and the phenyl radical source have been reported previously [37]. Briefly, a supersonic beam of helium-seeded phenyl radicals ( $C_6H_5$ ,  $X^2A_1$ ) at fractions of about 0.1% was generated in the primary

\* Corresponding author.

E-mail address: [ralfk@hawaii.edu](mailto:ralfk@hawaii.edu) (R.I. Kaiser).

**Table 1**  
Peak velocities ( $v_p$ ), speed ratios ( $S$ ), center-of-mass angle ( $\theta_{\text{CM}}$ ), and the collision energies ( $E_c$ ) of the phenyl radical with 1,2-butadiene.<sup>a</sup>

	$v_p$ , $\text{ms}^{-1}$	$S$	$E_c$ , $\text{kJ mol}^{-1}$	$\theta_{\text{CM}}$
$\text{C}_6\text{H}_5$ ( $X^2A_1$ )	$2496 \pm 28$	$4.5 \pm 0.2$	$109 \pm 3$	$12.6 \pm 0.5$
$\text{C}_6\text{H}_5$ ( $X^2A_1$ )	$3033 \pm 49$	$7.9 \pm 0.4$	$156 \pm 5$	$10.4 \pm 0.5$
1,2- $\text{C}_4\text{H}_6$ ( $X^1A'$ )	$794 \pm 25$	$5.9 \pm 0.8$	–	–

<sup>a</sup> Refers to the crossing segments.

source chamber via flash pyrolysis of nitrosobenzene ( $\text{C}_6\text{H}_5\text{NO}$ , Fluka) [38] employing a modified Chen source [39]. The mixture of the helium carrier gas and the nitrosobenzene vapor was released by a piezoelectric pulsed valve operated at a rate of 200 Hz and a backing pressure 920 Torr and passes a heated silicon carbide tube (1200–1500 K). At these experimental conditions, the decomposition of nitrosobenzene to form nitrogen monoxide (NO) and the phenyl radical ( $\text{C}_6\text{H}_5$ ) was quantitative [38]. After passing a skimmer, a part of the phenyl radical beam was selected by a four-slot chopper wheel. This section of the beam crossed perpendicularly a pulsed supersonic beam of 1,2-butadiene ( $\text{H}_2\text{CCC}(\text{CH}_3)\text{H}$ ;  $X^1A'$ ) (Fluka, 550 Torr) generated in the secondary source chamber. The peak velocities and speed ratios of the crossing segments of the beams are listed in Table 1.

The reactively scattering products were detected in the time-of-flight (TOF) mode by a rotatable quadrupole mass spectrometric detector after electron impact ionization of the neutral reaction products. The detector could be rotated inside the main chamber and within the plane defined by both supersonic beams. After recording TOF spectra at several angles and integrating them, a laboratory angular distribution (LAB) of the reactively scattered

species at a defined mass-to-charge ( $m/z$ ) ratio was derived. By fitting the TOF spectra and LAB angular distribution of products, the center-of-mass (CM) angular distribution  $T(\theta)$  and product translational energy distribution  $P(E_T)$  was obtained utilizing a forward-convolution routine [40–42]. Best fits were derived with an entrance barrier ( $E_0$ ) to the reaction of about 10–20  $\text{kJ mol}^{-1}$  incorporating an energy dependent cross section,  $\sigma(E_c)$ , of the form  $\sigma(E_c) \sim [1 - E_0/E_c]$ , via the line-of-center model with the collision energy  $E_c$  for  $E_c \geq E_0$  [43].

### 3. Results

#### 3.1. Laboratory data

In our experiments, TOF spectra were recorded at mass-to-charge ratios,  $m/z$ , of 130 ( $\text{C}_{10}\text{H}_{10}^+$ ), 129 ( $\text{C}_{10}\text{H}_9^+$ ), 128 ( $\text{C}_{10}\text{H}_8^+$ ), 117 ( $\text{C}_9\text{H}_9^+$ ), 116 ( $\text{C}_9\text{H}_8^+$ ), and 115 ( $\text{C}_9\text{H}_7^+$ ). It is important to emphasize that at both collision energies, the TOF spectra at different  $m/z$  values showed *identical* pattern and could be fitted with same center-of-mass functions. Therefore, signal at lower  $m/z$  ions originates solely from dissociation ionization of the parent molecule ( $\text{C}_{10}\text{H}_{10}$ ) in the electron impact ionizer of the detector. Further, we can conclude that the phenyl radical versus hydrogen atom pathway is open; upper limits to the methyl loss channel to form  $\text{C}_9\text{H}_8$  isomer(s) were derived to be up to 8%. Due to the best signal-to-noise ratio, time-of-flight data were recorded at a mass-to-charge ratio of  $m/z = 129$ , which is a fragment of the  $\text{C}_{10}\text{H}_{10}$  parent molecule generated in the reaction of phenyl radicals with 1,2-butadiene (Figs. 1 and 2). We would like to stress that due to the high background noise level at  $m/z = 78$  ( $^{13}\text{CC}_5\text{H}_5^+$ ) from the inelastically scattered phenyl radical reactant, the bimolecular hydrogen

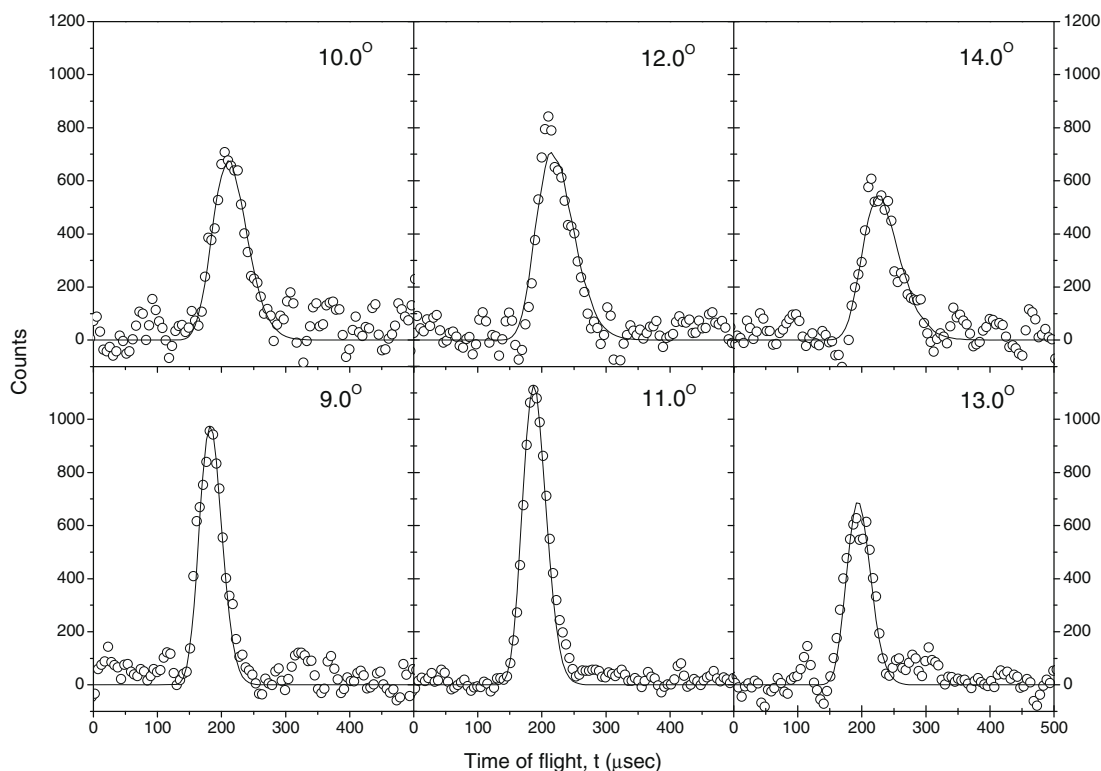


**Fig. 1.** Selected time-of-flight data recorded at mass-to-charge ratio ( $m/z = 129$ ), which is a fragment of the  $\text{C}_{10}\text{H}_{10}$  parent molecules generated in the reaction of phenyl radicals with 1,2-butadiene, at two collision energies of 109  $\text{kJ mol}^{-1}$  (upper row) and 150  $\text{kJ mol}^{-1}$  (lower row). The open circles are the experimental data, and the solid lines are the fits by forward-convolution routine.

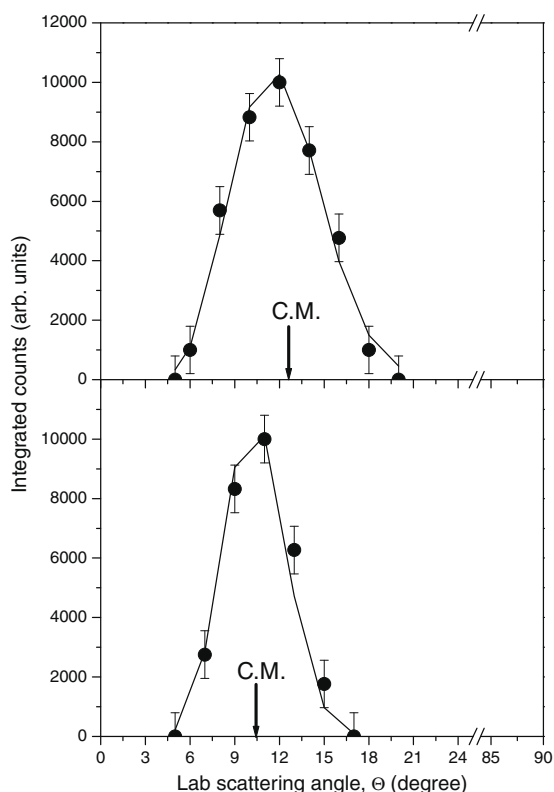


**Fig. 2.** Laboratory angular distributions of ion counts recorded at  $m/z = 129$  ( $C_{10}H_9^+$ ) in the reaction of phenyl radical with 1,2-butadiene at collision energy  $109 \text{ kJ mol}^{-1}$  (upper) and  $156 \text{ kJ mol}^{-1}$  (lower). The solid circles are the experimental data, and the solid lines are the fits. C.M. defines the center-of-mass angle.

abstraction pathway to form benzene ( $C_6H_6$ ) was undetectable. By integrating the TOF spectra at each angle and accounting for the data accumulation times, we were also able to derive the laboratory angular distributions of signal recorded at  $m/z = 129$  ( $C_{10}H_9^+$ ) (Fig. 2). Both LAB distributions are very narrow and spread over about  $15^\circ$  in the scattering plane defined by the phenyl radical and 1,2-butadiene beams.

### 3.2. Center-of-mass translational energy, $P(E_T)$ s, and angular distributions, $T(\theta)$ s

Based on the time-of-flight data alone, we have provided evidence on the formation of a  $C_{10}H_{10}$  isomer plus an atomic hydrogen formed via the bimolecular reaction of the phenyl radical and 1,2-butadiene. To extract meaningful information on the reaction dynamics and on the mechanism(s), the laboratory data (Figs. 1 and 2) are transformed into the center-of-mass frame. This provides the center-of-mass angular  $T(\theta)$  and translational energy  $P(E_T)$  distributions (Fig. 3). It is important to stress that at both collision energies, the TOF data (Fig. 1) and LAB distributions (Fig. 2) could be fit with a single channel. Let us have a look at the derived center-of-mass translational energy distributions,  $P(E_T)$ s, first. Best fits were obtained with distributions extending to maximum translational energy releases,  $E_{T,max}$ , of  $155 \pm 20$  and  $175 \pm 20 \text{ kJ mol}^{-1}$  for the lower and higher collision energies, respectively. Recall that the high-energy cutoffs present the sum of the absolute energy of the reaction plus the collision energy; this allows us to determine the reaction energy experimentally to be  $-46 \pm 20 \text{ kJ mol}^{-1}$  and  $-19 \pm 20 \text{ kJ mol}^{-1}$  at collision energies of  $109 \pm 3 \text{ kJ mol}^{-1}$  a  $156 \pm 5 \text{ kJ mol}^{-1}$ , respectively. On average, this

would account for a reaction energy of  $-33 \pm 25 \text{ kJ mol}^{-1}$ . We also observe that the center of mass translational energy distributions depict pronounced maxima at about  $30\text{--}50 \text{ kJ mol}^{-1}$ . This finding likely indicates the involvement of a tight exit transition state upon the formation of the  $C_{10}H_{10}$  isomer(s). Considering the principle of microscopic reversibility of a chemical reaction, the reverse reaction of hydrogen atom addition to the  $C_{10}H_{10}$  isomer is therefore expected to have an entrance barrier.

Secondly, it is important to analyze the center-of-mass angular distributions. It is evident that at both collision energies, the angular flux distributions show intensity over the complete angular range from  $0^\circ$  to  $180^\circ$ ; further, both distributions are asymmetric around  $90^\circ$  and depict enhanced fluxes in the forward hemispheres with respect to the phenyl radical beam. Best fits were derived with ratios at the poles,  $I(180^\circ)/I(0^\circ)$ , of  $0.4\text{--}0.7$ . What conclusions can be drawn from these findings? First, the flux present over the complete angular range strongly indicates that the reaction follows indirect scattering dynamics via the formation of  $C_{10}H_{11}$  reaction intermediate(s). Further, the asymmetry of the center-of-mass angular distributions let us conclude that the lifetime(s) of the  $C_{10}H_{11}$  intermediate(s) is shorter than (or comparable with) its rotational period (osculating complex).

## 4. Discussion

We now combine our experimental data with new electronic structure calculations on the reactions of phenyl radicals with 1,2-butadiene performed at the  $G3(MP2,CC)//B3LYP/6\text{--}311G^{**}+ZPE(B3LYP/6\text{--}311G^{**})$  level of theory [44] using the GAUSSIAN 98 [45] and MOLPRO 2002 [46] program packages. First, we compare the experimentally derived energetics to form the  $C_{10}H_{10}$  isomer ( $-46 \pm 20 \text{ kJ mol}^{-1}$  and  $-19 \pm 20 \text{ kJ mol}^{-1}$  at collision energies of  $109 \pm 3 \text{ kJ mol}^{-1}$  a  $156 \pm 5 \text{ kJ mol}^{-1}$ , respectively; average reaction energy of  $-33 \pm 25 \text{ kJ mol}^{-1}$ ) with the computed ones (Fig. 4). It is important to stress that the formation of both methyldiene isomers (**p3** and **p4**) can be ruled out since the computed reaction energies of  $166$  and  $153 \text{ kJ mol}^{-1}$  do not correlate with our experimental data. However, within the error limits, both the synthesis of 1-phenyl-3-methylallene (**p1**) ( $-33 \text{ kJ mol}^{-1}$ ) and 1-phenyl-butylene-2 (**p2**) ( $-24 \text{ kJ mol}^{-1}$ ) can account for the experimentally derived reaction energy of  $-33 \pm 25 \text{ kJ mol}^{-1}$ . Which is the dominating reaction product? Or are both isomers likely to be formed? To answer this question, we have to shed light on the underlying dynamics of the reaction. First, the indirect nature of the reaction mechanism to form **p1** and/or **p2** is evident from the shapes of the center-of-mass angular distributions (Fig. 3). If we also correlate the structure of the reactants with those of the final product isomers **p1** and/or **p2**, we can suggest that the phenyl radical adds with its radical center to the sterically less hindered C1 atom of the 1,2-butadiene molecule forming a doublet radical intermediate. In 1,2-butadiene, the carbon atoms involved in the double bonds have charges about  $-0.26$ ,  $0.00$ , and  $-0.20$ . Therefore, the attack is preferentially directed to the carbon atoms with the highest electron density, the terminal carbon atom C1. The larger cone of acceptance of the sterically less hindered, non-substituted carbon atom was found to be the more accessible pathway for the initial addition step of the phenyl radical in related reactions with methyl-substituted unsaturated hydrocarbons methylacetylene ( $CH_3CCH$ )<sup>25</sup> and propylene ( $CH_3C_2H_3$ ) [23]. Our electronic structure calculations support the proposed reaction mechanism (Fig. 4) and suggest that the phenyl radical adds via a barrier of about  $8 \text{ kJ mol}^{-1}$  to the C1 carbon atom of 1,2-butadiene forming intermediate **i1**; this structure is bound by  $154 \text{ kJ mol}^{-1}$  with respect to the separated reactants. The intermediate can decompose via atomic hydrogen loss from the C1 and C3 carbon atoms to yield **p1** and **p2** via tight exit transition states

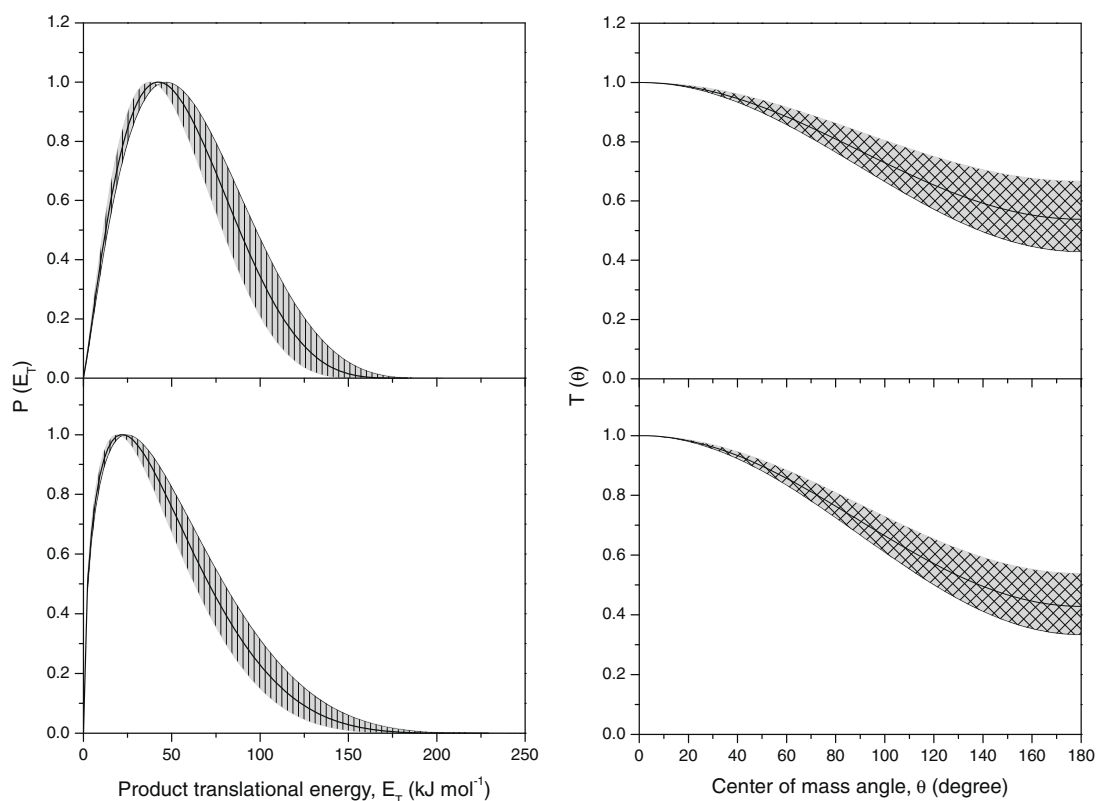


**Fig. 3.** Center-of-mass translational energy  $P(E_T)$ s (left) and angular  $T(\theta)$ s (right) distributions of the  $C_{10}H_{10}$  products formed in the reaction of phenyl radical with 1,2-butadiene at  $109 \text{ kJ mol}^{-1}$  (upper row) and  $156 \text{ kJ mol}^{-1}$  (lower row). The hatched areas account for the experimental error limits of the TOF spectra (Fig. 1) and laboratory angular distribution (Fig. 2) as well as the error limits of peak velocities and speed ratios of both supersonic beams (Table 1).

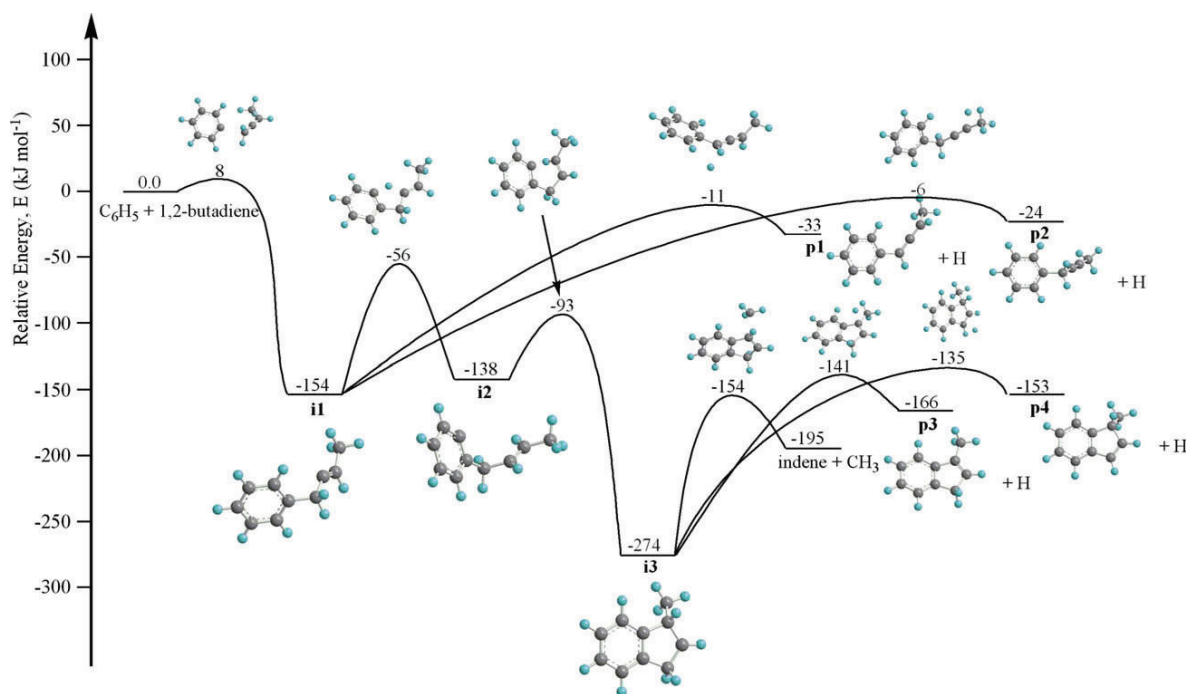


**Fig. 4.** Potential energy surface for the reaction of phenyl radicals with 1,2-butadiene calculated at the  $G3(MP2,CC)//B3LYP/6-311G^{**}+ZPE(B3LYP/6-311G^{**})$  level of theory.

located  $22 \text{ kJ mol}^{-1}$  and  $18 \text{ kJ mol}^{-1}$  above the final reaction products. The presence of tight exit transition states, which are con-

nected with a significant change in electron density from the intermediate to the final products, is also evident from the off-zero

peaking of the center-of-mass translational energy distributions (Fig. 3). On the other hand, the experimental data verify that under the present experimental conditions, intermediate **i1** does not rearrange via **i2** to **i3** yielding indene plus methyl or methylindene isomers plus atomic hydrogen. This leads us to the conclusion that the life time of **i1** is too low to allow an isomerization via hydrogen migration to **i2** followed by ring closure to **i3**. Quantitatively spoken, we can also estimate the life time of intermediate **i1** [47] taking into account of the moments of inertia of  $I_A = 0.269 \times 10^{-44} \text{ kg m}^2$ ,  $I_B = 1.344 \times 10^{-44} \text{ kg m}^2$ , and  $I_C = 1.402 \times 10^{-44} \text{ kg m}^2$  and the intensity ratios of the poles of the center-of-mass angular distributions,  $I(180^\circ)/I(0^\circ)$ , of 0.4–0.7. This suggests life times of the intermediate **i1** are about 0.21–0.54 ps, 0.87–2.68 ps, or 0.91–2.80 ps if rotating around its A, B, or C axis. This finding correlates nicely with the related reaction of phenyl radicals with 1,3-butadiene – an isomer of 1,2-butadiene – studied in our laboratory at collision energies of 117 and 149  $\text{kJ mol}^{-1}$  [24]. Here, the phenyl radical was also found to add to the C1 atom of 1,3-butadiene yielding a doublet reaction intermediate. The latter decomposed via hydrogen atom emission to the 1-phenyl-1,3-butadiene product rather than undergoing hydrogen shift and ring closure processes.

Having established an indirect reaction mechanism via a phenyl radical addition to the sterically less hindered, terminal carbon atom (C1) of the 1,2-butadiene reactant to form a doublet reaction intermediate **i1**, we still have to elucidate if isomer **p1** and/or **p2** are the final reaction products. Recall that the experimentally derived reaction energies and the proposed reaction mechanism can account for the formation of **p1** and/or **p2**. Let us compare the derived dynamics of the present reaction with those of related systems studied at similar collision energies in our laboratory. The reaction of phenyl radicals with methylacetylene led – via addition to the C1 carbon atom – to a  $\text{C}_6\text{H}_5\text{HCCCH}_3$  intermediate which decomposed to phenylmethylacetylene ( $\text{C}_6\text{H}_5\text{CCCH}_3$ ) plus atomic hydrogen. At collision energies between 91 and 161  $\text{kJ mol}^{-1}$ , the lifetime of the reaction intermediate was found to be too low to allow an ‘energy flow’ from the initially activated bond to the acetylenic carbon–hydrogen bond forming the phenylallene molecule via hydrogen loss from the acetylenic group to occur. On the other hand, the enhanced life time of the  $\text{C}_6\text{H}_5\text{H}_2\text{CCHCH}_3$  intermediate formed in the reaction of phenyl radicals with propylene allowed an energy randomization and ‘flow’ from the activated carbon–carbon bond to the carbon–hydrogen bonds in the methyl group; this resulted in the formation of two structural isomers: *cis/trans*-1-phenylpropene ( $\text{CH}_3\text{CHCHC}_6\text{H}_5$ ) (80–90%) and 3-phenylpropene ( $\text{H}_2\text{CCHCH}_2\text{C}_6\text{H}_5$ ). The enhanced life time of the  $\text{C}_6\text{H}_5\text{H}_2\text{CCHCH}_3$  intermediate (phenyl – propylene reaction) compared to the  $\text{C}_6\text{H}_5\text{HCCCH}_3$  intermediate (phenyl – methylacetylene reaction) was attributed to the increased numbers of vibration modes of the reaction intermediates. This in turn allowed an energy ‘flow’ from the initially activated bond to the carbon–hydrogen bond rupture of in the methyl group of the propylene reactant. This qualitative concept leads us to predict that in the initial reaction intermediate **i1** ( $\text{C}_6\text{H}_5\text{H}_2\text{CCHCH}_3$ ), which contains an even increased number of oscillators compared to the  $\text{C}_6\text{H}_5\text{H}_2\text{CCHCH}_3$  intermediate (phenyl – propylene reaction), two reaction pathways are open: the ejection of the hydrogen atom from the C1 carbon atom (energy flow via only one bond) yielding **p1** and also an emission of the hydrogen atom from C3 (energy flow via three chemical bonds).

## 5. Conclusions

The reaction of the phenyl radical with 1,2-butadiene was studied under single collision conditions in a crossed molecular beams machine. Combining the experimental data with electronic struc-

ture calculations, the reaction follows indirect scattering dynamics via an addition of the phenyl radical with its radical center to the sterically more favorable C1 atom of the 1,2-butadiene reactant. This intermediate decomposed via atomic hydrogen loss to form most likely two  $\text{C}_{10}\text{H}_{10}$  isomers: the 1-phenyl-3-methylallene (**p1**) and 1-phenyl-butyne-2 (**p2**) isomers via tight exit transition states in overall exoergic reactions. Compared to the reaction of phenyl radicals with 1,3-butadiene, which resulted in the formation of 1-phenyl-1,3-butadiene, two structurally very distinct isomers were formed. Since both 1,3-butadiene and 1,2-butadiene isomers and the phenyl radical reactant have been monitored in combustion flames of hydrocarbon fuel [48], we can predict that the 1-phenyl-1,3-butadiene, 1-phenyl-3-methylallene, and 1-phenyl-butyne-2 isomers should be present in sooting hydrocarbon flames as well. It remains to be established in future experiments to what extent these molecules can isomerize via hydrogen atom catalyzed reactions to the thermodynamically more stable methylindene isomers.

## Acknowledgements

This work was supported by the US Department of Energy, Basic Energy Sciences (DE-FG02–03ER15411 to the University of Hawaii and DE-FG02–04ER15570 to Florida International University).

## References

- [1] J.L. Weisman, A. Mattioda, T.J. Lee, D.M. Hudgins, L.J. Allamandola, C.W. Bauschlicher Jr., M. Head-Gordon, *Phys. Chem. Chem. Phys.* 7 (2005) 109.
- [2] B.N. Pappas, S. Wang, N.J. DeYonker, H.L. Woodcock, H.F. Schaefer III, *J. Phys. Chem. A* 107 (2003) 6311.
- [3] M.P. Bernstein, S.A. Sandford, L. Allamandola, *J. Astrophys.* 472 (1996) L127.
- [4] C.X. Mendoza-Gomez, M.S.d. Groot, J.M. Greenberg, *Astron. Astrophys.* 295 (1995) 479.
- [5] D.M. Hudgins, C.W. Bauschlicher Jr., L.J. Allamandola, J.C. Fetzer, *J. Phys. Chem. A* 104 (2000) 3655.
- [6] S.P. Ekern, A.G. Marshall, J. Szczepanski, M.J. Vala, *Phys. Chem. A* 102 (1998) 3498.
- [7] B.J. Finlayson-Pitts, J.N. Pitts, *Science* 276 (1997) 1045.
- [8] K.J. Hylland, *Toxicol Environ. Health A* 69 (2006) 109.
- [9] J.H. Seinfeld, J.F. Pankow, *Ann. Rev. Phys. Chem.* 54 (2003) 121.
- [10] J.L. Durant, W.F. Busby, A.L. Lafleur, B.W. Penman, C.L. Crespi, *Mutat. Res. Genet. Toxicol.* 371 (1996) 123.
- [11] A.W. Wood et al., *Cancer Res.* 40 (1980) 642.
- [12] P.P. Fu, F.A. Beland, S.K. Yang, *Carcinogenesis* 1 (1980) 725.
- [13] W.F. Busby Jr., E.K. Stevens, E.R. Kellenbach, J. Cornelisse, J. Lugtenburg, *Carcinogenesis* 9 (1988) 741.
- [14] E. Dwek et al., *Astrophys. J. Lett.* 475 (1997) 565.
- [15] Y.J. Pendleton, L.J. Allamandola, *Astrophys. J. Suppl. Ser.* 138 (2002) 75.
- [16] W.W. Duley, *Faraday Discuss.* 133 (2006) 415.
- [17] E. Peeters, A.L. Mattioda, D.M. Hudgins, L.J. Allamandola, *Astrophys. J.* 617 (2004) L65.
- [18] D. Romanini, L. Biennier, F. Salama, A. Kachanov, L.J. Allamandola, F. Stoeckel, *Chem. Phys. Lett.* 303 (1999) 165.
- [19] M. Hausmann, K.H. Homann, in: *International Annual Conference of ICT 1991*, 22nd (Combust. React. Kinet.) 1991, 22/1.
- [20] M.E. Law, P.R. Westmoreland, T.A. Cool, J. Wang, N. Hansen, C.A. Taatjes, T. Kasper, *Proc. Combust. Inst.* 31 (2007) 565.
- [21] H. Richter, J.B. Howard, *Prog. Energy Combust. Sci.* 26 (2000) 565.
- [22] F. Zhang, X. Gu, Y. Guo, R.I. Kaiser, *J. Organic Chem.* 72 (2007) 7597.
- [23] F. Zhang, X. Gu, Y. Guo, R.I. Kaiser, *J. Phys. Chem. A* 112 (2008) 3284.
- [24] X. Gu, F. Zhang, R.I. Kaiser, *J. Phys. Chem. A* 113 (2009) 998.
- [25] X. Gu, F. Zhang, Y. Guo, R.I. Kaiser, *J. Phys. Chem. A* 111 (2007) 11450.
- [26] X. Gu, F. Zhang, Y. Guo, R.I. Kaiser, *Angew. Chem. Int. Ed.* 46 (2007) 6866.
- [27] F. Zhang, X. Gu, R.I. Kaiser, *J. Chem. Phys.* 128 (2008) 084315/1.
- [28] L. Letendre, D.K. Liu, C.D. Pibel, J.B. Halpern, H.L. Dai, *J. Chem. Phys.* 112 (2000) 9209.
- [29] X. Mu, I.-C. Lu, S.-H. Lee, X. Wang, X. Yang, *J. Chem. Phys.* 121 (2004) 4684.
- [30] H.-Y. Lee, V.V. Kislov, S.-H. Lin, A.M. Mebel, D.M. Neumark, *Chem. Eur. J.* 9 (2003) 726.
- [31] Y. Hidaka, T. Higashihara, N. Ninomiya, T. Oki, H. Kawano, *Int. J. Chem. Kinet.* 27 (1995) 331.
- [32] S.D. Chambreaux, J. Lemieux, L. Wang, J. Zhang, *J. Phys. Chem. A* 109 (2005) 2190.
- [33] N. Balucani, H.Y. Lee, A.M. Mebel, Y.T. Lee, R.I. Kaiser, *J. Chem. Phys.* 115 (2001) 5107.
- [34] R.D. Kern, H.J. Singh, C.H. Wu, *Int. J. Chem. Kinet.* 20 (1988) 731.

- [35] Y. Hidaka, T. Higashihara, N. Ninomiya, H. Masaoka, T. Nakamura, H. Kawano, *Int. J. Chem. Kinet.* 28 (1996) 137.
- [36] Y. Wang, W. Feng, M. Lei, R. Liu, *Sci. China Ser. B: Chem.* 41 (1998) 60.
- [37] X. Gu, Y. Guo, F. Zhang, A.M. Mebel, R.I. Kaiser, *Faraday Discuss.* 133 (2006) 245.
- [38] R.I. Kaiser, O. Asvany, Y.T. Lee, H.F. Bettinger, P.v.R. Schleyer, H.F. Schaefer III, *J. Chem. Phys.* 112 (2000) 4994.
- [39] D.W. Kohn, H. Clauberg, P. Chen, *Rev. Sci. Instrum.* 63 (1992) 4003.
- [40] M.S. Weiss, Ph.D. Thesis, University of California, Berkeley, 1986.
- [41] M. Vernon, Ph.D. Thesis, University of California, Berkeley, 1981.
- [42] R.I. Kaiser et al., *Faraday Discuss.* 119 (2001) 51.
- [43] R.D. Levine, *Molecular Reaction Dynamics*, Cambridge University Press, Cambridge, 2005.
- [44] L.A. Curtiss, K. Raghavachari, P.C. Redfern, A.G. Baboul, J.A. Pople, *Chem. Phys. Lett.* 314 (1999) 101.
- [45] M.J. Frisch, *GAUSSIAN 98*, Revision A. 11, Gaussian, Inc., Pittsburgh, PA, 2001.
- [46] MOLPRO, a package of ab initio programs designed by H.-J. Werner, P.J. Knowles, version 2002.1. R.D. Amos, A. Bernhardsson, A. Berning, P. Celani, D.L. Cooper, M.J.O. Deegan, A.J. Dobbyn, F. Eckert, C. Hampel, G. Hetzer, P.J. Knowles, T. Korona, R. Lindh, A.W. Lloyd, S.J. McNicholas, F.R. Manby, W. Meyer, M.E. Mura, A. Nicklass, P. Palmieri, R. Pitzer, G. Rauhut, M. Schutz, U. Schumann, H. Stoll, A.J. Stone, R. Tarroni, T. Thorsteinsson, H.-J. Werner.
- [47] W.B. Miller, S.A. Safron, D.R. Herschbach, *Discuss. Faraday. Soc.* 44 (1967) 108.
- [48] H. Bockhorn, *Soot Formation in Combustion: Mechanisms and Models*, Springer, Berlin, 1994.